

Scattering of Carriers by Magnetic Mn Impurities in PbTe: Mn Alloys

G. Toth and J. Y. Leloup

Laboratoire B. P. Grégory, Ecole Polytechnique, Paris, France

and

H. Rodot

*Laboratoire de Magnétisme et de Physique des Solides,
Centre National de la Recherche Scientifique, Meudon-Bellevue, France*

(Received 22 December 1969)

The carrier mobility and the spin exchange between carriers and localized magnetic Mn impurities are studied in *p*-type PbTe:Mn alloys. Using helicon propagation, the mobility measurements lead to a value for the total manganese impurity cross section $\sigma_{\text{scatt}} = 5 \times 10^{-16} \text{ cm}^2$. The linewidth of the Mn electron spin resonance is studied as a function of temperature, number of carriers, and manganese concentration. The carrier-dependent linewidth is explained in terms of a Korringa mechanism. From this analysis, the exchange constant $J = 0.07 \text{ eV}$ is deduced. From this value of J , the spin-flip scattering cross section $\sigma_{\text{sf}} = 4 \times 10^{-19} \text{ cm}^2$ is calculated.

I. INTRODUCTION

In the last few years, there has been a rising interest in the problem of magnetic impurities dissolved in various matrices. In particular, the interaction between localized moments and conduction electrons in metallic dilute alloys has been extensively studied.¹ Recently, preliminary work has been carried out in semiconductors with the main idea that one can modify an important parameter, the Fermi energy, by varying the carrier concentration. The first alloys that have been studied with this purpose are GeTe: Mn, SnTe: Mn, and PbTe: Mn.^{2,3} However, the impurity concentrations used were too large to be able to observe anomalies on the resistivity and on the magnetization analogous to those already seen in the case of localized moments in metals.

We have studied *p*-type alloys of PbTe: Mn by electron spin resonance (ESR) and transport methods. For the transport measurements, we used a rf method (helicon wave propagation) which gives the mobility of the bulk material. From the mobility measurements, we deduce the total scatter-

ing cross section of the manganese impurity. The spin exchange interaction J is responsible for the ESR linewidth due to the carriers. From the deduced value of J , we calculate the spin-flip part of the cross section.

II. SAMPLE PREPARATION AND EXPERIMENTAL TECHNIQUES

The alloys were prepared from PbTe and MnTe with purities of 99.9999%. In order to avoid the formation of manganese oxide, the MnTe was introduced into the final ingot through a master alloy of MnTe and PbTe. The method we used to obtain single crystals was the following: A zone melting with a very thin zone (5–10 mm) and low speed (1 mm/h) was conducted on an ingot of PbTe along which a measured quantity of powder of the master alloy was homogeneously scattered. This method provides good solid solutions, which are homogeneous a few centimeters away from each end of the ingot, and avoids segregation.

Samples of $6 \times 4 \times 2 \text{ mm}^3$ were wire cut and electrolytically etched so that at least 300μ were re-

TABLE I. Concentrations and peak-to-peak experimental linewidths (in G) of the five samples studied.

Sample	Mn concentration (in ppm)	Carrier concentration (in cm^{-3})	Linewidth at		
			4.2 °K	77 °K	300 °K
No. 10	150	3.4×10^{18}	7	20	... ^a
No. 12	500	1.2×10^{18}	10	17	30
No. 9	1350	3.7×10^{18}	14	27	60
No. 11	2000	1.2×10^{19}	17.5	42	... ^b
No. 8	3000	3.2×10^{18}	22.5	36	65

^aThe line was not seen at 300 °K because of the small Mn content.

^bAs explained in the text, the line of sample 11 was too broad to be seen.

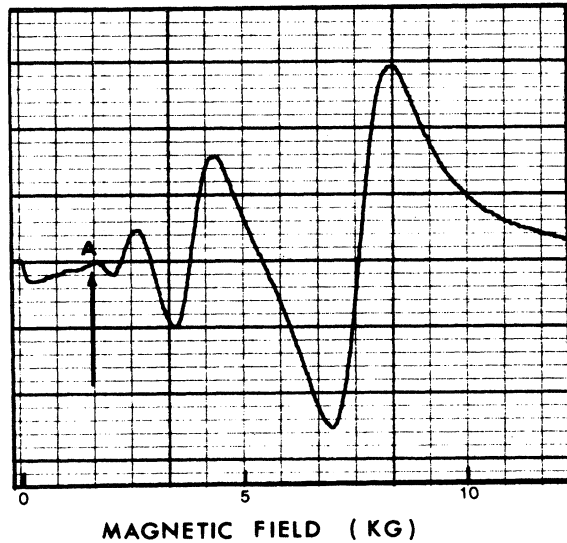


FIG. 1. Typical helicon resonance curve at 4.2°K. Point A shows the onset of the resonances.

moved from the surface to erase all traces of mechanical treatment.

Table I lists the concentrations of the samples we studied. The number of carriers was determined by helicon dimensional resonance and the manganese concentration by an electron microprobe⁴ and chemical analysis. We found that the carrier concentration is independent of the quantity of manganese present. The manganese is neither a donor nor an acceptor, showing that the Mn energy levels do not lie in the gap.

The measurements were performed on a conventional 10-GHz ESR spectrometer and on a nuclear magnetic spectrometer previously used for helicon experiments⁵ with a frequency range of 2–16 MHz.

III. PRESENTATION AND INTERPRETATION OF EXPERIMENTAL RESULTS

A. Resistivity and Impurity Cross Section

Pure PbTe has a very low resistivity at low temperatures ($\approx 10^{-5}$ Ω cm) due to the high mobility of the carriers, over 10^6 $\text{cm}^2/\text{V sec}$ for the best crystals. In our samples, the mobility is significantly lower (2×10^4 to 2×10^5 $\text{cm}^2/\text{V sec}$). The mobility is deduced from helicon dimensional resonances⁶ which exist under certain conditions. Consider a slab of thickness t in which helicon waves can propagate. The calculation of the complex helicon impedance leads to two limiting cases for t larger or smaller than the helicon penetration depth δ . In the case $t \gg \delta$, the helicon wave penetrates only a little into the sample and there are no resonances. In the other case $t \ll \delta$, there are resonances when the sample contains a half-integer

number of wavelengths. Since helicon waves only exist when a large dc magnetic field is applied, there will be an onset of the resonances for a given magnetic field (see point A in Fig. 1). This onset is ruled by a condition of the form $\omega_c \tau \approx 1$. However, as explained in Ref. 6, the precise condition at point A is

$$\omega_c \tau = q \frac{1}{2} \pi, \quad (1)$$

where q is an integer such that $2q + 1$ is the number of half-wavelengths contained in the sample. Thus, from Eq. (1) we obtain a value of τ and, hence, of the mobility. The accuracy of the absolute values for the mobility is approximately $\pm 20\%$. However, this method determines directly the mobility, and, being a rf method, avoids the difficulty of soldering electrodes and of measuring very low resistivities.

The mobility is plotted on Fig. 2 versus the Mn concentration. These results show that the mobility is limited by the manganese impurities, at least for concentrations above a few hundred ppm. We can therefore calculate the corresponding scattering cross section from⁷

$$\sigma_{\text{scatt}} = (\pi/3)^{1/3} (2e/h)(1/\mu N n^{1/3}), \quad (2)$$

where μ is the mobility, N the impurity concentration, and n the carrier density. We find the value $\sigma_{\text{scatt}} = 5 \times 10^{-18}$ cm^2 .

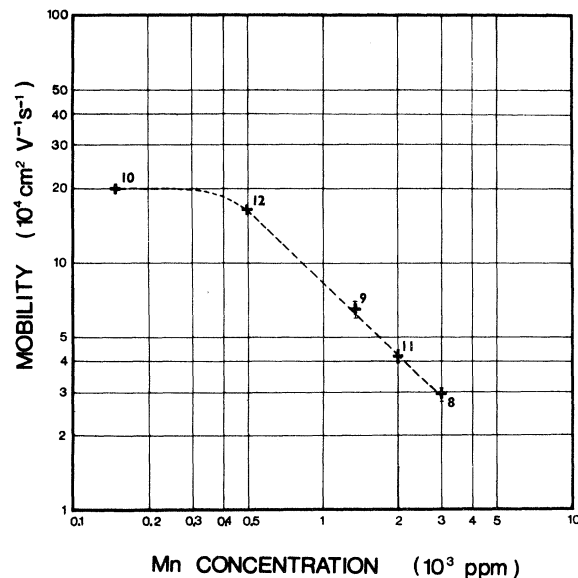


FIG. 2. Carrier mobility at 4.2°K, as deduced from the abscissa of point A of Fig. 1. The mobility, except for very low Mn content, is limited by manganese scattering as shown by the -1 slope of the line. The numbers on the figure refer to the samples of Table I.

B. ESR and Spin-Flip Cross Section

The ESR experiments were performed to measure quantitatively the weak exchange interaction between the carriers and the manganese impurities. The six lines of the Mn hyperfine structure have already been seen in Mn-doped PbTe, PbSe, and PbS; however, when it was seen, emphasis was put on PbSe: Mn and on the effect of the matrix on the localized electronic wave function using g -shift measurements.⁸ In the present work, we study the exchange interaction between the carrier and localized electron spins by measuring the ESR linewidth as a function of carrier concentration and temperature.

The experimental data is shown in Table I. The linewidth increases with temperature. At low temperatures (4.2 °K), one sees that the linewidth is controlled by the Mn concentration; whereas, for higher temperatures, the Mn concentration is not the important parameter. In the following, we will show that, at 77 and 300 °K, the carrier concentration is the dominant factor. At 300 °K, there are rather large uncertainties in the determination of the linewidths because they are of the order of the hyperfine splitting. For sample 11, with the highest concentration of carriers, the lines completely vanish.

To interpret our results we distinguish three

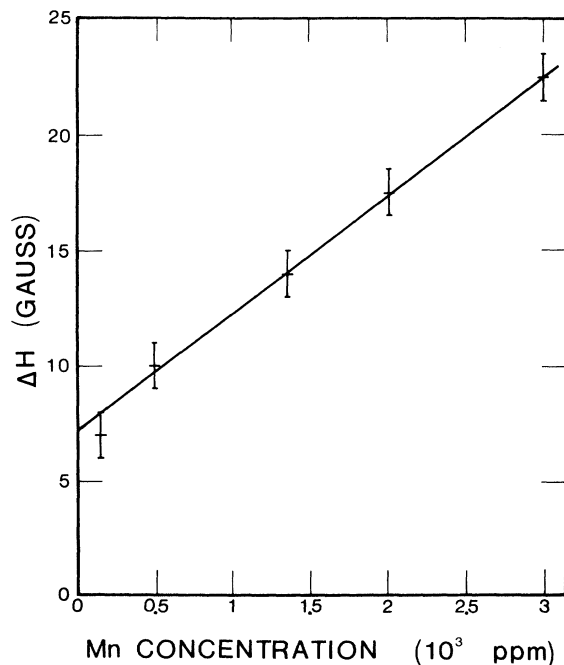


FIG. 3. ESR linewidth measurements at 4.2 °K. At this temperature, there is no contribution due to the carriers and we see the effect of the Mn-Mn dipolar broadening on the Mn resonance line.

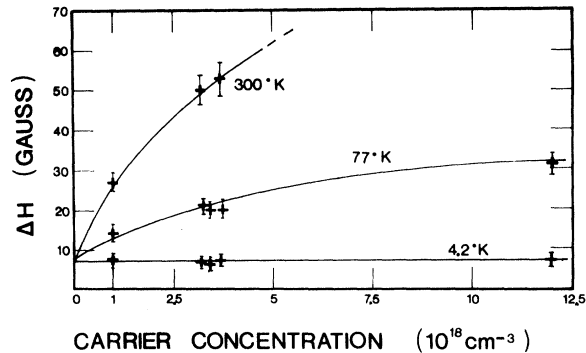


FIG. 4. Linewidth for several temperatures versus carrier concentration after subtraction of the Mn-Mn dipolar broadening. As shown by the three intermediate samples, which have very different Mn concentrations, the linewidth depends only on carrier concentration. The curve is the calculated one, using the Korringa relation [Eq. (3)] and the value for J of 0.07 eV. The above fit is thus obtained with J as the only adjustable parameter.

contributions to the linewidth: (i) the width of a single Mn atom in a PbTe matrix (excluding the effect of the carriers), (ii) the Mn-Mn dipolar broadening, and (iii) the width due to the effect of the carriers, which we shall study in detail.

(i) *Linewidth of a single Mn atom.* In Fig. 3, the measured linewidths at 4.2 °K are plotted versus the manganese concentration. The experimental points fit well on a straight line which extrapolates to a value of approximately 7 G. This extrapolated linewidth is mainly due to the hyperfine interaction with neighboring nuclei and does not vary very much with temperature.

(ii) *Linewidth due to the dipolar broadening.* At 4.2 °K, the effect of the carriers on the linewidth is very small; therefore, we will neglect their presence. The linear dependence (Fig. 3) of the linewidth on Mn concentration is explained by a Mn-Mn dipolar coupling. To obtain the contribution due to the dipolar broadening, we subtract the extrapolated width of 7 G. This dipolar contribution is in complete agreement with the calculated one using the moments method.⁹ It is noted that the impurity concentrations of our samples fall well within the limit of high dilution where the dipolar broadening is proportional to the concentration rather than to the square root of the concentration.

(iii) *Linewidth due to the carriers.* We have subtracted the dipolar broadening from the experimental linewidths and plotted the results in Fig. 4. As we discussed above, the remaining width at 4.2 °K is that of a single Mn atom. We will attribute the increase of the linewidth at 77 and 300 °K to the carriers. This carrier-dependent linewidth depends only on carrier concentration as exempli-

fied by the three samples (samples 8, 9, and 10 in Table I), with almost the same carrier density, which have nearly the same linewidth although they have quite different Mn concentrations.

We interpret the dependence of the linewidth on carrier concentration (Fig. 4) and its increase with temperature in terms of a Korringa relaxation mechanism via a spin-exchange interaction between localized electrons and carriers. We write the spin-exchange part of the Hamiltonian as $J\vec{S}\cdot\vec{s}(\vec{r})$ where \vec{S} is the impurity spin and $\vec{s}(\vec{r})$ the carrier spin density. The PbTe: Mn alloys contain two sets of spins: One set is attached to the electrons on the Mn impurities with a g factor of 2, the other one to the conduction holes with a g factor varying between 15 and 57 depending on crystalline orientation.¹⁰ The two sets of spins are coupled by the exchange interaction $J\vec{S}\cdot\vec{s}(\vec{r})$. This situation of two systems of spins with quite different g values is very similar to the relaxation of nuclei by conduction electrons in metals where the contact Hamiltonian $A\vec{I}\cdot\vec{S}$ is responsible for the relaxation. The relaxation time is obtained from the Korringa formula¹¹

$$1/T_1 = (64\pi/\hbar)J^2[\rho(E_F)]^2 kT \quad (3)$$

The condition of application of the Korringa mechanism to the problem of the relaxation of electronic localized spins by carriers is discussed in the Appendix.

The carrier density $\rho(E_F)$ has to be calculated for each sample and each temperature; we used the formulas given by Sapoval¹² which take into account the corrections for temperature and non-parabolicity of the band. Thus, with $\rho(E_F)$ and Eq. (3) we obtain a value of J corresponding to each experimental point of Fig. 4. The entire experimental data is well explained by the value $J = 0.07 \pm 0.01$ eV.

From this value of J we compute the spin-flip scattering cross section due to the $J\vec{S}\cdot\vec{s}(\vec{r})$ term in the Hamiltonian from¹³

$$\sigma_{sf} = (3/2\hbar)(n/v_F E_F)J^2 S(S+1) \quad (4)$$

Since the Fermi velocity v_F is not isotropic, we have calculated an upper limit for σ_{sf} by taking the smallest value for v_F . We find $\sigma_{sf} = 4 \times 10^{-19}$ cm².

IV. CONCLUSION

Our measurements give precise data for the scattering of carriers by manganese impurities in PbTe. We have measured the total scattering cross section of a manganese impurity and the spin-flip part of this cross section. The total scattering cross section ($\sigma_{scatt} = 5 \times 10^{-16}$ cm²) is small, of the order of atomic dimensions; it has the same value as that of several nonmagnetic

donor impurities, for which the measured value is 4×10^{-16} cm².¹⁴ Another point to be noted is that manganese is not a dopant in PbTe. Furthermore, we studied the spin exchange between localized electrons and carriers by measuring its effect on the ESR linewidth. We measured the exchange constant $J = 0.07 \pm 0.01$ eV. This leads to a value of the spin-flip scattering cross section ($\sigma_{sf} = 4 \times 10^{-19}$ cm²) three orders of magnitude smaller than that of σ_{scatt} . Electron spin resonance was the adequate tool to measure such a small spin-flip scattering cross section. The consequence is that we feel there is little hope of observing the effect of the spin exchange on transport properties.

ACKNOWLEDGMENTS

The authors gratefully acknowledge the constant help and guidance of Professor I. Solomon. They also wish to thank B. Sapoval and D. Kaplan for many illuminating discussions.

APPENDIX

In this Appendix, we attempt to clarify the validity of using a Korringa mechanism to explain the observed linewidth.

The physical picture is that of two systems of spins placed in a magnetic field \vec{H} with resonant frequencies ω_s for the carriers and ω_d for the localized spins. As long as the exchange coupling between these two systems is small compared to the energy difference $\hbar(\omega_d - \omega_s)$, one can apply a perturbation treatment which is precisely the Korringa calculation. This condition can be expressed as $1/\tau_s < \omega_d - \omega_s$, τ_s being the lifetime of a carrier spin due to the exchange interaction.

Furthermore, the longitudinal and transverse relaxation times are equal in this case because of the very short correlation time associated with the Korringa relaxation process.

When the g factors of the two systems of spins become approximately equal, or more precisely when the exchange coupling becomes large compared to the energy difference $\hbar(\omega_d - \omega_s)$, a perturbation treatment is no longer valid. This is the case of dilute magnetic impurities in metals. This case has been treated by Hasegawa,¹⁵ whose model leads to a set of phenomenological equations in which the transverse magnetization of the two spin systems are coupled, whereas in the "Korringa case", they are not. This coupling leads to effects such as the "bottleneck effect" found by Gossard *et al.*¹⁶ Such effects cannot occur in our case because of the absence of a coupling between the transverse magnetizations of the impurity and the carrier spins.

- ¹M. D. Daybell and W. A. Steyert, *Rev. Mod. Phys.* **40**, 380 (1968).
- ²J. E. Lewis and M. Rodot, *J. Phys. (Paris)* **29**, 352 (1968).
- ³J. Cohen, A. Globa, P. Mollard, H. Rodot, and M. Rodot, *J. Phys. (Paris)* **29**, 142 (1968).
- ⁴R. Castaing, *Advances in Electronics and Electron Physics* (Academic, New York, 1961), Vol. XIII, p. 317.
- ⁵B. Sapoval, *Phys. Rev. Letters* **17**, 241 (1966).
- ⁶C. R. Legédy, *Phys. Rev.* **135**, A1713 (1964).
- ⁷R. S. Allgaier and W. W. Scanlon, *Phys. Rev.* **111**, 1029 (1958).
- ⁸J. H. Pifer, *Phys. Rev.* **157**, 272 (1967).
- ⁹A. Abragam, *The Principles of Nuclear Magnetism* (Oxford U. P., Oxford, England, 1961), Chap. IV.
- ¹⁰C. K. N. Patel and R. E. Slusher, *Phys. Rev.* **177**, 1200 (1969).

- ¹¹The factor 64 instead of 4 in the Korringa formula arises from the shape of the Fermi surface of PbTe (four ellipsoids centered at the L points of the Brillouin zone in the four equivalent $\langle 111 \rangle$ directions). The probabilities of a simultaneous electron-electron spin flip involves wave vectors belonging either to the same ellipsoid or to two adjacent ones (intravalley or intervalley processes). We thus get 16 equivalent terms provided that we take for $\rho(E_F)$ the density of states for each ellipsoid.
- ¹²B. Sapoval, *J. Phys. (Paris)* **29**, 133 (1968).
- ¹³Z. Béal-Monod and R. A. Weiner, *Phys. Rev.* **170**, 552 (1968).
- ¹⁴Y. Kanai, R. Nii, and N. Watanabe, *J. Appl. Phys.* **32**, 2146 (1961).
- ¹⁵H. Hasegawa, *Progr. Theoret. Phys. (Kyoto)* **21**, 483 (1959).
- ¹⁶A. C. Gossard, A. J. Heeger, and J. H. Wernick, *J. Appl. Phys.* **39**, 1251 (1967).

Electrical Resistivity due to Dislocations*

A. B. Bhatia and O. P. Gupta[†]

Theoretical Physics Institute, Physics Department, University of Alberta, Edmonton, Canada
(Received 26 January 1970)

Regarding a dislocation as a row of weak scatterers, each having spherically symmetric potential, a solution of the linearized Boltzmann equation in the presence of a set of parallel dislocations is obtained. The method consists of expanding the distribution function in terms of spherical harmonics and, as developed here, it is exact for the monovalent metals. For polyvalent metals there are additional contributions to the resistivity tensor which arise from the diffraction peaks which occur when the electron wavelength is smaller than twice the interatomic distance – these terms are estimated by the variational method. By allowing for other mechanisms (impurities) of scattering to be present, it is found that the dislocation resistivity ρ_D depends on the resistivity due to other mechanisms also. Numerical results for these deviations from Matthiessen's rule and for ρ_D for randomly oriented dislocations in aluminum are obtained by taking, after Harrison, the scatterers constituting the dislocations to be vacancies.

I. INTRODUCTION

This paper is mainly concerned with the problem of solving the Boltzmann transport equation, and hence calculating the electrical resistivity, for a set of parallel dislocations treating each dislocation to be a row of weak scatterers each having a spherically symmetric potential. Such an investigation is desirable for several reasons.

First, the preliminary investigation made by Harrison¹ show that, though crude, the above model is not far from reality and it is of interest to obtain a reliable estimate of the resistivity on its basis. Parenthetically, it may be recalled that the calculations,²⁻⁴ which consider the electron scattering to arise primarily from the elastic strain field associated with a dislocation, give values for

the resistivity which are at least an order of magnitude smaller than the observed values. Second, if our solution is extended to the case where the potential due to the individual scatterers is allowed to have radial asymmetry in the plane perpendicular to the row, the model would simulate the scattering due to an exact arrangement of the ions near the core of an edge dislocation.⁵ Third, an exact solution, if only for a simple model, is important because it can be used as a guide to the reliability of the various approximate procedures which have been in use – or, if one wants to use the variational technique, for constructing a suitable trial function.

The scattering probability of an electron due to a dislocation is anisotropic, i. e., it depends not only on the relative orientation of the incident and